Diffusion of Organic Dyes in Immobilized and Free Catanionic Vesicles

Shantanu Dey, Ujjwal Mandal, Supratik Sen Mojumdar, Amit Kumar Mandal, and Kankan Bhattacharyya*

Department of Physical Chemistry, Indian Association for the Cultivation of Science, Jadavpur, Kolkata 700 032, India

Received: July 22, 2010; Revised Manuscript Received: September 18, 2010

Fluorescence correlation spectroscopy (FCS) has been used to study the motion of fluorescent dyes in a giant (diameter 20 000 nm = 20 μm) catanionic vesicle comprised of the surfactant sodium dodecyl sulfate (SDS) and dodecyltrimethyl ammonium bromide (DTAB). The diffusion in the anion (SDS) rich catanionic vesicle was studied both in bulk water and in an immobilized vesicle attached to a positively charged glass surface. In the case of the immobilized vesicle, the diffusion coefficients (D_t) of R6G (rhodamine 6G), DCM (4-dicyanomethylene-2-methyl-6-*p*-dimethyl aminostyryl-4*H*-pyran), and C343 (coumarin 343) are found to be 1.5, 2.5, and 10 $\mu m^2/s$, respectively, which are 280, 120, and 55 times slower compared to those for the same dyes in bulk water. The magnitude of D_t is found to vary for different vesicles. This was attributed to the difference in size and shape of the immobilized vesicles. In bulk, R6G binds completely to the vesicle and exhibits extremely slow diffusion with $D_t = 0.5 \pm 0.1$ $\mu m^2/s$ (~850 and 3 times slower compared to that of R6G in bulk water and within the immobilized vesicle). This is attributed to very slow overall diffusion of the very large size vesicles (20 μm = 20 000 nm). Both of the dye molecules (DCM and C343) show two different diffusion coefficients for the vesicles in bulk. In this case, the small D_t (0.5 ± 0.1 $\mu m^2/s$) corresponds to the diffusion of the vesicle as a whole and the large D_t value (300 and 550 $\mu m^2/s$ for DCM and C343, respectively) corresponds to the free dye molecules in bulk water.

1. Introduction

In recent years, fluorescence correlation spectroscopy (FCS) has been applied to study the diffusion of a single molecule in a liquid or in many organized assemblies.[1−13] This includes micelles,[1] microemulsions,[2] vesicles and membranes,[3−5] colloidal particles,[6] agarose gel,[8] polymer gel,[9a] and supramolecular complexes[9b] and studies of protein aggregation.[10] Using far-field microscopy, Moerner et al. recorded the Brownian motion of a single dye molecule in a polyacrylamide gel.[7] Molecular diffusion in lipid membranes is fundamental in protein dynamics, transfection of nucleic acids into cells, and, hence, functions of living cells. Lipid layer topography related local modification in diffusion and interaction with membranes has significant biological and physical ramifications. The ensemble averaged studies in bulk solutions do not, in general, reveal the microscopic fluctuations in an individual system. Natural systems (e.g., proteins or membranes) exhibit significant structural, spatial, and conformational heterogeneity. The role of heterogeneity in energy transfer in light harvesting proteins,[4a] ion channel proteins,[4b] and enzymatic reactions[4c] has recently been elucidated by single molecule spectroscopy.

In principle, it is not possible to spatially resolve different regions of dimension ~20 nm in a microscope of spatial resolution ~200 nm (for 405 nm excitation). To circumvent this limitation, we used three dyes of different polarities which will be localized in different regions of a heterogeneous system. Previously, we have applied this strategy to study spatial heterogeneity (region dependence) of the diffusion coefficient (D_t) in the micelle and gel phase of a triblock copolymer.[12] In this case, the gel consists of interpenetrating micellar aggregates of diameter ~20 nm.[14] A hydrophobic dye, DCM, is located at the core of the micelle or gel, while the anionic dye C343 prefers the hydrophilic corona region. These three probes exhibit similar D_t in bulk water (300 $\mu m^2/s$ for DCM, 550 $\mu m^2/s$ for C343, and 600 $\mu m^2/s$ for C480). In the gel, when the motion of an individual micelle is suppressed, the three dyes exhibit very different D_t values. The D_t value of the hydrophobic dye DCM in the gel (D_t ~1 $\mu m^2/s$) is 29 times smaller than that of the hydrophilic dye C343 (D_t ~29 $\mu m^2/s$).[12] It is proposed that the hydrophobic DCM "walks" through the interpenetrating polymer chain while hydrophilic C343 remains in the water filled "void" inside the gel. In other words, the hydrophobic probe (DCM) and the hydrophilic probe (C343) report diffusion in different regions.

Most recently, we have studied the region dependence and phase dependence of D_t in lipid vesicles.[11] In the gel phase of the lipid vesicle (1,2-dipalmitoyl-*sn*-glycero-3-phosphocholine, DPPC), the translational diffusion of the hydrophobic fluorescent dye DCM (D_t ~5 $\mu m^2/s$) is found to be ~8 times smaller than that in the fluid phase (D_t ~40 $\mu m^2/s$) of the lipid (1,2-dilauroyl-*sn*-glycero-3-phosphocholine, DLPC).[11] In a lipid (DPPC), the hydrophobic dye DCM (D_t ~5 $\mu m^2/s$) diffuses ~8 times more slowly than the hydrophilic dye, C343 (D_t ~40 $\mu m^2/s$). This is attributed to different locations of the hydrophobic dye (DCM) and the hydrophilic dye (C343). Finally, we observed significant variation in the magnitude of D_t that varies for individual vesicles of the same constitution. This is ascribed to the fluctuations in size and shape of the vesicle.

The interaction of the cationic surfactant (dodecyl trimethyl ammonium bromide, DTAB) with an anionic surfactant (sodium dodecyl sulfate, SDS) results in the formation of a catanionic vesicle.[15] Using cryo-transmission electron microscopy (TEM), Kaler et al. showed that at a DTAB/SDS ratio 37.5:62.5 the

* To whom correspondence should be addressed. E-mail: pckb@iacs.res.in. Fax: (91)-33-2473-2805.

10.1021/jp1068347
Published on Web 11/05/2010

SCHEME 1: Schematic Representation of (A) Coumarin 343 (C343), (B) DCM, and (C) Rhodamine 6G (R6G)

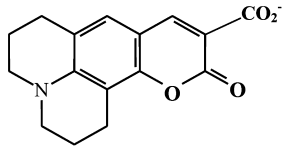

(A) C343

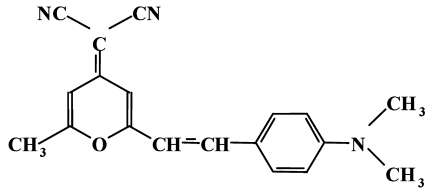

(B) DCM

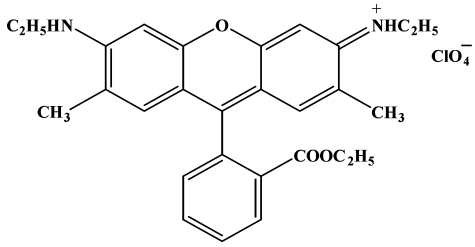

(C) R6G

system contains mainly unilamellar vesicles (dimension ~100 nm) with a few multilamellar vesicles of very large size (~10 μm = 10 000 nm). The structure and dynamics of SDS−DTAB catanionic vesicles (SDS rich) have been studied in bulk using dynamic light scattering (DLS) and femtosecond spectroscopy.[16] In the present work, we apply FCS to study the translational diffusion of a fluorescence probe in a SDS−DTAB catanionic vesicle. Note that a study carried out in the bulk probes an ensemble of vesicles of different sizes. In this work, we focus on diffusion of a fluorescent dye molecule in a single giant vesicle of diameter 20 00 nm. Since the catanionic vesicles do not stick to an ordinary glass surface, we used a modified (positively charged) glass surface to immobilize the vesicles. To probe diffusion in different regions of the cationic vesicle, we used three fluorescent probes, C343 (anionic), DCM (neutral), and R6G (cationic). We will show that there is a marked variation in the translational diffusion coefficient (D_t) of the three dyes in the immobilized vesicles.

Recently, English et al. used FCS to study the interaction of DNA with catanionic vesicles.[5] They reported that the organic solutes and DNA adsorbed electrostatically to the exterior surface of oppositely charged catanionic vesicles through interaction with unpaired ionic surfactants present in the vesicle bilayer. Using FCS, they showed that the surfactant concentration affects the vesicle bilayer composition. They also observed that negatively charged DNA binds much more strongly to the exterior surface of positively charged catanionic vesicles and the binding of DNA stabilizes vesicles at very low surfactant concentrations.[5]

2. Experimental Section

Laser grade dyes, coumarin 343 (C343, Scheme 1A), 4-dicyanomethylene-2-methyl-6-*p*-dimethyl aminostyryl-4*H*-pyran (DCM, Scheme 1B), and rhodamine 6G (R6G, Scheme 1C), were used as received from Exciton Inc. An equivalent amount of potassium hydroxide (KOH) was added with C343 in order to obtain its anionic form. Sodium dodecyl sulfate (SDS) and dodecyltrimethyl ammonium bromide (DTAB) were purchased from Aldrich and used without further purification.

For the catanionic vesicle, we have chosen a narrow region of the phase diagram.[15a] Requisite amounts of SDS and DTAB were first dissolved in a 1:2 solvent mixture of $CHCl_3$ and MeOH. A solution containing the solvents was completely evaporated by heating in a water bath at 70 °C. Finally, distilled water is added to form a catanionic vesicle. The aqueous solution of the vesicle contained 0.625 wt % SDS and 0.375 wt % DTAB. This composition is chosen to ensure the formation of large vesicles as reported earlier.[15a]

For the modification of the glass surface, at first the coverslips (Gold Seal, USA) were rinsed in acetone and sonicated in a classical ultrasonic bath (EYELA, Japan) for 30 min in 1 M aqueous KOH solution. Then, the coverslips were rinsed five times with Milli-Q water. The washed coverslips were then placed in a reaction flask containing 100 mL of MeOH, 5 mL of acetic acid, and 1 mL of amino propyl silane (APS). Then, the reaction container was stirred well and kept for 1 h. Finally, the coverslips were washed with Milli-Q water again and dried to afford an APS modified glass surface.

The dye samples were studied by FCS using a confocal microscope (PicoQuant, MicroTime 200) with an inverted optical microscope (Olympus IX-71). A water immersion objective (60×, 1.2 NA) was used to focus the excitation light (405 nm) from a pulsed diode laser on the sample placed on a coverslip. After collecting the fluorescence via the same objective, it was allowed to pass through a dichroic mirror and appropriate band-pass filters. We used an HQ430LP filter to block the exciting light (405 nm). To detect the fluorescence, suitable bandpass filters (HQ480/40M for C343 and HQ580/70M for DCM and R6G) were used. The fluorescence was then focused through a pinhole (50 μm) and eventually on a beam splitter prior to entering the two single photon counting avalanche photodiodes (SPADs). The fluorescence cross-correlation traces were recorded using two detectors (SPADs). The signal was subsequently processed by the PicoHarp-300 time correlated single photon counting card (PicoQuant) to generate the cross correlation function, $G(\tau)$.

Data analysis of individual correlation curves was performed using the SymPhoTime software supplied by PicoQuant. The correlation function $G(\tau)$ of the fluorescence intensities is given by[13a]

$$G(\tau) = \frac{\langle \delta F(0) \delta F(\tau) \rangle}{\langle F \rangle^2} \tag{1}$$

where $\langle F \rangle$ is the average intensity and $\delta F(\tau)$ is the fluctuation in intensity at a delay τ around the mean value, i.e., $\delta F(\tau) = \langle F \rangle - F(\tau)$.

In order to fit the correlation functions, we used a 3D diffusion model having a triplet contribution (SymPho Time). For K fractions of dye diffusing within a system with distinct diffusion constants, the correlation function $G(\tau)$ is given by[13a,b]

$$G(\tau) = \frac{1 - T + T\exp(-\tau/\tau_{tr})}{N(1 - T)} \sum_{i=1}^{K} \phi_i (1 + \tau/\tau_i)^{-1} \times (1 + \tau/\tau_i S^2)^{-1/2} \tag{2}$$

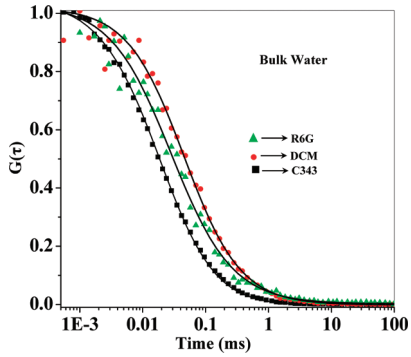

Figure 1. Normalized fluorescence cross correlation curves in water obtained by FCS for C343 (■), R6G (▲), and DCM (●). The points denote the actual values of $G(\tau)$, and the solid line denotes the best fit.

TABLE 1: Diffusion Coefficients (D_t) of the Dyes in Different Systems

system	diameter (nm)	D_t[a] ($\mu m^2/s$) of the dyes		
		C343	DCM	R6G
bulk water		550	300	426
SDS micelle	4	430	110	50
DTAB micelle	4	60	90	150

[a] ±5%.

In the above equation, τ_i denotes the average time a dye molecule resides in the confocal volume, τ_{tr} is the lifetime of a dye molecule in its triplet state, τ is the delay or the lag time, ϕ_i is the fractional weighting factor for the ith contribution to the autocorrelation function, N is the average number of molecules in the excitation volume, and T indicates the fraction of molecules in the triplet state. S ($=w_z/w_{xy}$) is the structure parameter of the excitation volume, and w_z and w_{xy} are the longitudinal and transverse radii, respectively. The structure parameter (S) of the excitation volume was calibrated using a sample (R6G in water) of known diffusion constant ($D_t = 426$ $\mu m^2/s$).[13c] The estimated volume of the excitation volume is ~0.8 fL with a transverse radius (w_{xy}) of ~305 nm. All of the FCS and microscopy measurements were done at 20 °C. The diffusion constant (D_t) was calculated (using the two-dimensional model) from the following equation:

$$\tau_i = \frac{w_{xy}^2}{4D_t} \tag{3}$$

From the calculated value of the diffusion constant (D_t), one can easily determine the hydrodynamic radius (r_h) of the diffusing species using the Stokes−Einstein equation

$$r_h = \frac{k_B T}{4\pi\eta_0 D_t} \tag{4}$$

3. Results and Discussion

3.1. Diffusion in Bulk Water. Figure 1 shows the temporal profile of the fluorescence correlation functions (FCS trace) of the three probes in bulk water. In bulk water, the coefficients of translational diffusion (D_t) of the three dyes (DCM, C343, and R6G) are found to be 300, 550, and 426 $\mu m^2/s$, respectively (Table 1 and Figure 1).

3.2. Diffusion in Micelles in Bulk. In this section, we discuss the diffusion of the three organic dyes in micelles in bulk water.

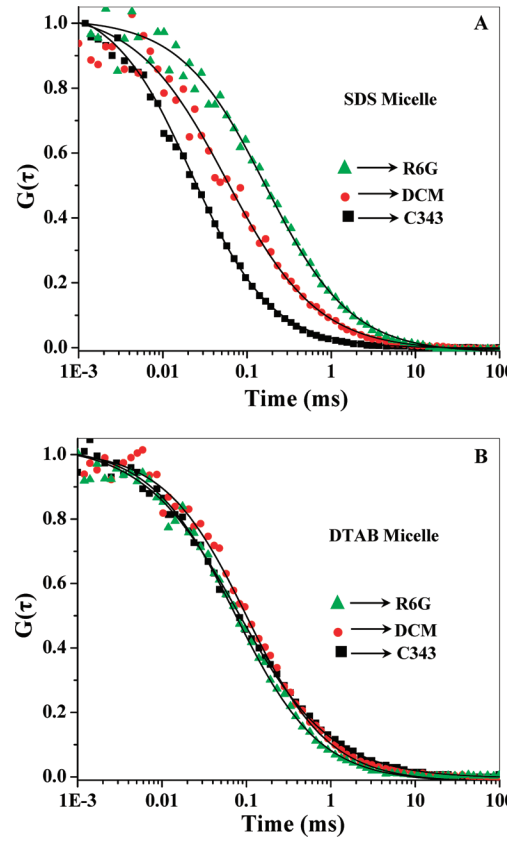

Figure 2. (A) Normalized fluorescence cross correlation curves of C343 (■), DCM (●), and R6G (▲) in SDS micelle ($\lambda_{ex} = 405$ nm). The points denote the actual values of $G(\tau)$, and the solid line denotes the best fit. (B) Normalized fluorescence cross correlation curves of C343 (■), DCM (●), and R6G (▲) in DTAB micelle ($\lambda_{ex} = 405$ nm). The points denote the actual values of $G(\tau)$, and the solid line denotes the best fit.

If the dyes bind firmly to the micelle, FCS reports motion of the micelle, and with the micelle being much larger than the molecules, this causes slow diffusion. Figure 2 shows the FCS data for the three dyes in the SDS and DTAB micelle. Since SDS is an anionic surfactant, the positively charged dye (R6G) binds electrostatically to the anionic micelle and displays a slow translational diffusion ($D_t = 50$ $\mu m^2/s$, Table 1). This is ~9 times smaller compared to that in bulk water. Similarly, in a cationic surfactant (DTAB), a negatively charged dye (C343) shows slow diffusion ($D_t = 60$ $\mu m^2/s$, Table 1). This is also 9 times smaller compared to that observed in bulk water (550 $\mu m^2/s$). The smaller diffusion of R6G in SDS micelle (50 $\mu m^2/s$) and C343 in DTAB micelle (60 $\mu m^2/s$) is ascribed to the movement of the micelle as a whole.

3.3. FCS in SDS−DTAB Vesicles Immobilized on a Positively Charged Glass Surface. In the absence of any dye molecule, the SDS−DTAB catanionic vesicles themselves do not emit any fluorescence. In the presence of dye, a large number of dye molecules assemble inside the vesicle and give rise to intense fluorescence emission. Figure 3 shows the confocal images of catanionic vesicles containing the R6G molecule adsorbed on the glass surface. Since the dye R6G is cationic, it binds well with the catanionic vesicle carrying a net negative charge. The confocal images were recorded at 10 min intervals for a period of 40 min. It is observed that the vesicles remain in the same position during this period. This confirms that the catanionic vesicles are immobilized on the positively charged glass surface and remain stationary during the duration of the experiment. Figure 4 shows the fluctuation of the fluorescence

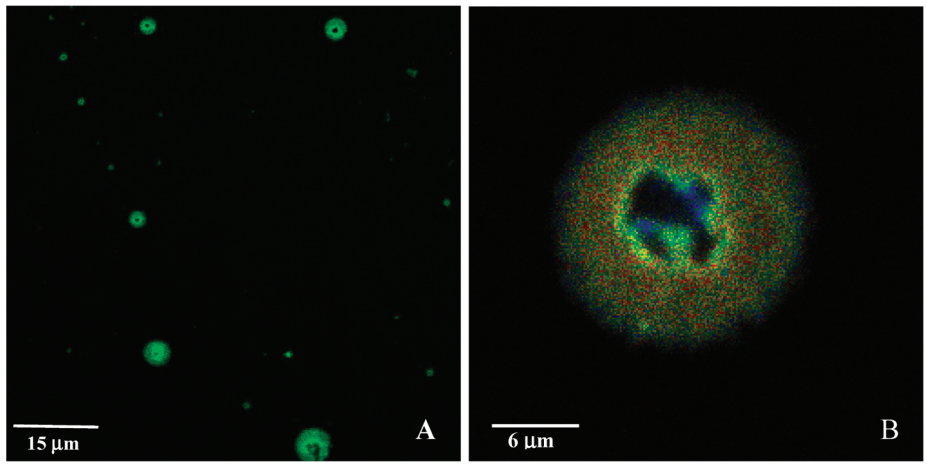

Figure 3. Confocal fluorescent images of single catanionic vesicles immobilized on a positive glass surface obtained by objective scanning at 20 °C. The image size is (A) 80 μm × 80 μm and (B) 30 μm × 30 μm. The vesicle contains ~1 nM C343.

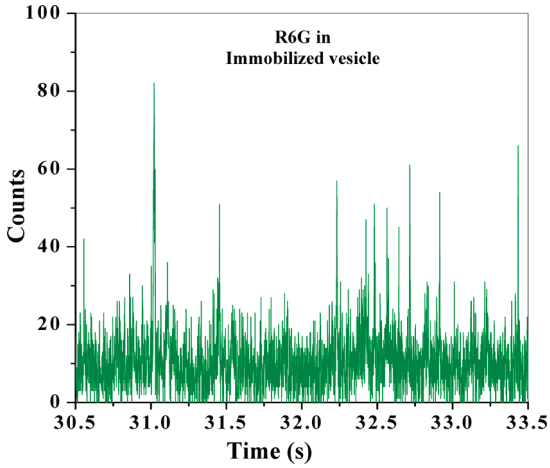

Figure 4. Typical fluorescence intensity−time record of fluorescence bursts of ~1 nM R6G in a SDS−DTAB catanionic vesicle.

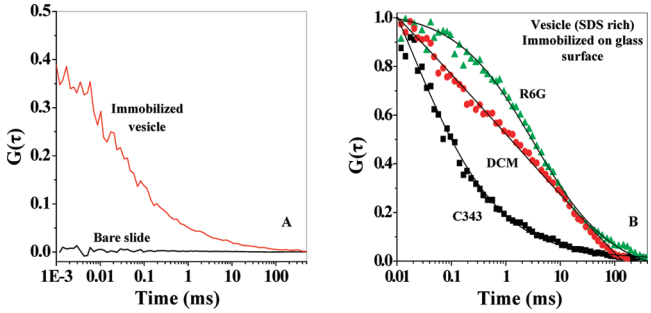

Figure 5. (A) Comparison of the cross correlation function obtained from C343 diffusing through a vesicle immobilized on a glass surface with that from a bare slide. (B) Normalized fluorescence cross correlation curves of C343 (■), DCM (●), and R6G (▲) in an immobilized SDS−DTAB catanionic vesicle (λ_{ex} = 405 nm). The points denote the actual values of $G(\tau)$, and the solid line denotes the best fit.

intensity of the R6G molecules inside the catanionic vesicle obtained by focusing the objective within the vesicle. It may be noted that the correlation curve obtained by focusing the laser beam on the vesicle is completely different from that of the bare slide. Figure 5A shows that there is no correlation when the laser beam is focused on the bare slide.

When the exciting laser beam was focused on the individual catanionic vesicle, we observed substantial slower diffusion of all three dyes. Note, since the beam focused (spatial resolution ~200 nm, much smaller than micrometer sized vesicles) on the

TABLE 2: Diffusion Coefficient (D_t) of the Dyes in SDS−DTAB (SDS Rich) Catanionic Vesicles

system	diameter (nm)	D_t (μm^2/s) of the dyes C343	DCM	R6G
vesicle immobilized on a positive glass surface	20 000	10[a]	2.5[a]	1.5[a]
bulk vesicle		0.5 (3%)[b] 550 (97%)[a]	0.5 (86%)[b] 300 (14%)[a]	0.5 (100%)[b]

[a] ±5%. [b] ±0.1.

vesicles (stationary), one observes diffusion of the fluorescent probe molecule inside the vesicle. In catanionic vesicles, the diffusion constant of R6G was found to be 1.5 μm^2/s (Table 2 and Figure 5B). This is ~280 times slower than that in bulk water. This suggests slow diffusion of R6G molecules inside the vesicle. The diffusion constants of DCM and C343 were found to be 2.5 and 10 μm^2/s, respectively (Figure 5B). The D_t values of DCM and C343 in catanionic vesicles are respectively ~120 times and ~55 times slower compared to that in bulk water.

The D_t values markedly vary for the individual catanionic vesicles immobilized on a glass surface. Figure 6 shows the distribution of D_t values of the three dyes in the catanionic vesicles immobilized on a positively charged glass surface. The distribution of D_t was fitted to a Gaussian, and the mean value was taken as the average. Such a distribution of D_t may arise from the variation in size and shape of the catanionic vesicles. The distribution in D_t demonstrates that the diffusion in a single vesicle is markedly different from that in the bulk where an ensemble is studied and one gets an ensemble average of D_t.

In summary, the translational diffusion of three dyes decreases markedly in the catanionic vesicle immobilized on a glass surface. The D_t values correspond to the motion of the dye molecules inside the vesicle. Positively charged dye R6G remains electrostatically attached to the anionic vesicle and shows very small D_t (1.5 μm^2/s). The anionic dye C343 remains relatively more mobile and displays higher D_t (10 μm^2/s). The neutral hydrophobic probe DCM remains at the core of the immobilized vesicle and displays a D_t value (2.5 μm^2/s) intermediate between that of the cationic probe R6G (1.5 μm^2/s) and anionic probe C343 (10 μm^2/s).

3.4. FCS in SDS−DTAB Vesicles: Bulk Diffusion. In this section, we discuss the diffusion of dye molecules in the same catanionic vesicle in the bulk and compare the result with immobilized vesicles attached on a positively charged glass

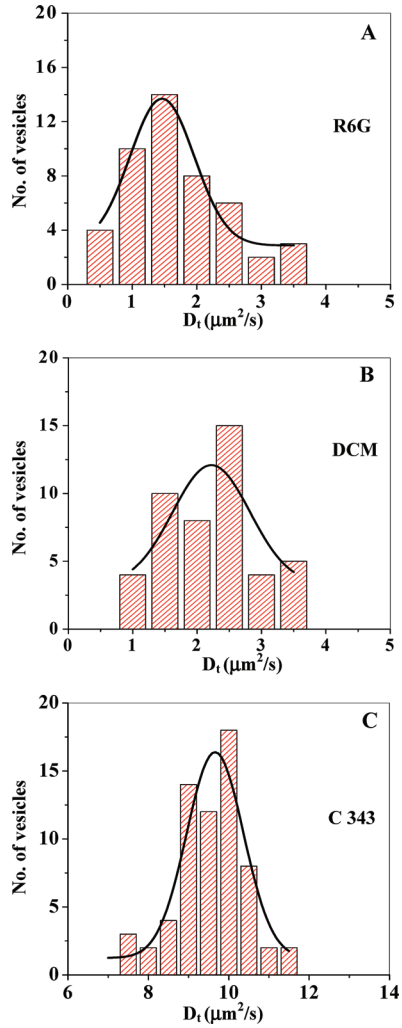

Figure 6. Distribution of D_t values obtained by analyzing ~50 individual SDS−DTAB vesicles for (A) R6G, (B) DCM, and (C) C343. The mean value of D_t was determined by fitting the distribution to a Gaussian.

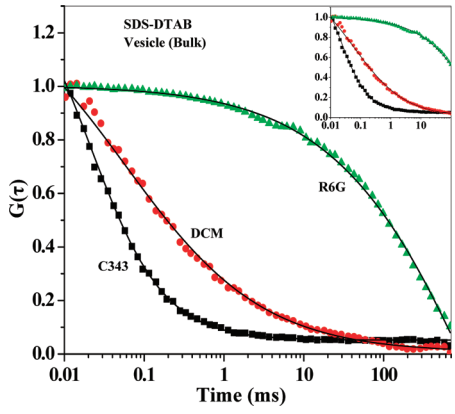

Figure 7. Normalized fluorescence cross correlation curves of C343 (■), DCM (●), and R6G (▲) in a bulk SDS−DTAB vesicle (λ_{ex} = 405 nm). The points denote the actual values of $G(\tau)$, and the solid line denotes the best fit.

surface. For this purpose, we have focused the laser beam in the bulk solution containing the vesicles. Figure 7 shows the FCS data for the three dyes in the bulk vesicle. In this case, R6G exhibits extremely slow diffusion with a diffusion coefficient of 0.5 ± 0.1 $\mu m^2/s$ (Table 2 and Figure 8) which is ~3 times slower than that in an immobilized vesicle (1.5 $\mu m^2/s$).

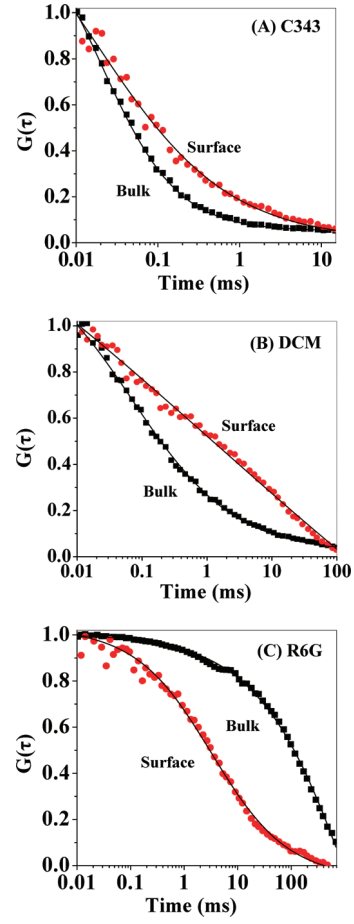

Figure 8. Normalized fluorescence cross correlation curves of (A) C343, (B) DCM, and (C) R6G in a bulk SDS−DTAB vesicle (■) and in an immobilized vesicle (●) (λ_{ex} = 405 nm). The points denote the actual values of $G(\tau)$, and the solid line denotes the best fit.

In the bulk, R6G remains fixed through electrostatic attraction with the vesicle and, hence, shows a very small D_t value (0.5 ± 0.1 $\mu m^2/s$). Previously, we detected D_t = 7 $\mu m^2/s$ for a 100 nm sized vesicle.[11] According to the Stokes−Einstein equation, a 20 μm (20 000 nm) sized vesicle is expected to show a D_t value of 0.02 $\mu m^2/s$. The observed D_t value of 0.5 ± 0.1 $\mu m^2/s$ indicates that, in the bulk, there is a significant contribution from freely diffusing vesicles which are much smaller than the 20 μm sized vesicle. It may be noted that a vesicle of diameter 1 μm roughly corresponds to an expected D_t value of 0.5 ± 0.1 $\mu m^2/s$. Thus, the D_t value of 0.5 ± 0.1 $\mu m^2/s$ indicates an ensemble average value of vesicles of different sizes.

In the bulk, DCM and C343 display two diffusion coefficients—a fast one for dye in bulk and a very slow one (D_t ~0.5 ± 0.1 $\mu m^2/s$) due to the diffusion of the vesicle as a whole. The neutral hydrophobic dye DCM exhibits two diffusion coefficients, 0.5 ± 0.1 $\mu m^2/s$ (86%) and 300 $\mu m^2/s$ (14%), respectively. The small D_t (0.5 ± 0.1 $\mu m^2/s$) corresponds to the diffusion of the vesicle as a whole and the large D_t (300 $\mu m^2/s$) for the free dye molecules in bulk water. The relative contribution of the DCM dyes in bulk water is very small (14%). The anionic dye C343 exhibits two diffusion coefficients, 0.5 ± 0.1 $\mu m^2/s$ (3%) and 550 $\mu m^2/s$ (97%). In this case, most of the free C343 dye molecules are present in bulk water (Figure 8). In the case of the positively charged dye, R6G, all of the dyes remained bound to the vesicle and we obtained only a slow component (0.5 ± 0.1 $\mu m^2/s$) for the diffusion of the vesicle. It seems that the slow diffusion of the vesicle in bulk suppresses observation of the motion of the individual dye molecules within a vesicle.

4. Conclusion

This work demonstrates a marked difference in the diffusion of dyes in an immobilized vesicle and in a bulk vesicle. In both cases, the three dyes exhibit very slow diffusion. In the case of an immobilized vesicle, the difference in D_t of the three dyes is ascribed to their charge (positive, negative, and neutral) and location (e.g., core for DCM). It is observed that there is a marked variation (fluctuation) of D_t values in the immobilized vesicle. The fluctuation of D_t values may be attributed to the different size and shape of the vesicles immobilized on the glass surface. The substantial slow diffusion ($D_t \sim 0.5 \pm 0.1$ $\mu m^2/s$) of R6G in bulk is due to overall motion of the vesicle as a whole. The dye molecules, DCM and C343, show two diffusion coefficients for a vesicle in the bulk. In this case, the slow diffusion coefficient (0.5 ± 0.1 $\mu m^2/s$) corresponds to the diffusion of the vesicle as a whole and the large diffusion constant ($300-550$ $\mu m^2/s$) arises from the diffusion of the dye molecules in bulk water.

Acknowledgment. Thanks are due to Department of Science and Technology, India (Project Number: IR/I1/CF-01/2002), J. C. Bose Fellowship, and Council of Scientific and Industrial Research (CSIR) for generous research grants. S.D., U.M., S.S.M., and A.K.M. thank CSIR for awarding fellowships.

References and Notes

(1) (a) Zettl, H.; Portnoy, Y.; Gottlieb, M.; Krausch, G. *J. Phys. Chem. B* **2005**, *109*, 13397. (b) Norenberg, R.; Klingler, J.; Horn, D. *Angew. Chem., Int. Ed.* **1999**, *38*, 1626. (c) Erhardt, R.; Zhang, M.; Boker, A.; Zettl, H.; Abetz, C.; Frederik, P.; Krausch, G.; Abetz, V.; Muller, A. H. E. *J. Am. Chem. Soc.* **2003**, *125*, 3260. (d) Colombani, O.; Ruppel, M.; Schubert, F.; Zettl, H.; Pergushov, D. V.; Muller, A. H. E. *Macromolecules* **2007**, *40*, 4338.

(2) Burnett, G. R.; Rees, G. D.; Steytler, D. C.; Robinson, B. H. *Colloids Surf., A* **2004**, *250*, 171.

(3) (a) Korlach, J.; Schwille, P.; Webb, W. W.; Feigenson, G. W. *Proc. Natl. Acad. Sci. U.S.A.* **1999**, *96*, 8461. (b) Benda, A.; Benes, M.; Marecek, V.; Lhotsky, A.; Hermens, W. Th.; Hof, M. *Langmuir* **2003**, *19*, 4120. (c) Humpolickova, J.; Gielen, E.; Benda, A.; Fagulova, V.; Vercammen, J.; vandeVen, M.; Hof, M.; Ameloot, M.; Engelborghs, Y. *Biophys. J.* **2006**, *91*, L23.

(4) (a) He, Y.; Zeng, X.; Mukherjee, S.; Rajapaksha, S.; Kaplan, S.; Lu, H. P. *Langmuir* **2010**, *26*, 307. (b) Harms, G. S.; Orr, G.; Montal, M.; Thrall, B. D.; Colson, S. D.; Lu, H. P. *Biophys. J.* **2003**, *85*, 1826. (c) Chen, Y.; Hu, D.; Vorpagel, E. R.; Lu, H. P. *J. Phys. Chem. B* **2003**, *107*, 7947.

(5) Lioi, B. S.; Wang, X.; Islam, M. R.; Danoff, D.; English, D. S. *Phys. Chem. Chem. Phys.* **2009**, *11*, 9315.

(6) Muller, C. B.; Loman, A.; Richtering, W.; Enderlein, J. *J. Phys. Chem. B* **2008**, *112*, 8236.

(7) Dickson, R. M.; Norris, D. J.; Tzeng, Y.-L.; Moerner, W. E. *Science* **1996**, *274*, 966.

(8) (a) Fatin-Rouge, N.; Wilkinson, K. J.; Buffle, J. *J. Phys. Chem. B* **2006**, *110*, 20133. (b) Fatin-Rouge, N.; Starchev, K.; Buffle, J. *Biophys. J.* **2004**, *86*, 2710.

(9) (a) Michelman-Ribeiro, A.; Boukari, H.; Nossal, R.; Horkay, F. *Macromolecules* **2004**, *37*, 10212. (b) Yue, H.; Wu, M.; Xue, C.; Velayudham, S.; Liu, H.; Waldeck, D. H. *J. Phys. Chem. B* **2008**, *112*, 8218. (c) Zettl, H.; Hafner, W.; Boker, A.; Schmalz, H.; Lanzendorfer, M.; Muller, A. H. E.; Krausch, G. *Macromolecules* **2004**, *37*, 1917.

(10) (a) Sahoo, B.; Balaji, J.; Nag, S.; Kaushalya, S. K.; Maiti, S. *J. Chem. Phys.* **2008**, *129*, 075103. (b) Schubert, F.; Zettl, H.; Hafner, W.; Krauss, G.; Krausch, G. *Biochemistry* **2003**, *42*, 10288.

(11) Ghosh, S.; Adhikari, A.; Sen Mojumdar, S.; Bhattacharyya, K. *J. Phys. Chem. B* **2010**, *114*, 5736.

(12) Ghosh, S.; Mandal, U.; Adhikari, A.; Bhattacharyya, K. *Chem. Asian J.* **2009**, *4*, 948.

(13) (a) Lakowicz, J. R. *Principles of Fluorescence Spectroscopy*, 3rd ed.; Springer: New York, 2006; Chapter 24. (b) Brock, R.; Hink, M. A.; Jovin, T. M. *Biophys. J.* **1998**, *75*, 2547. (c) Petrasek, Z.; Schwille, P. *Biophys. J.* **2008**, *94*, 1437.

(14) Wanka, G.; Hoffman, H.; Ulbricht, W. *Macromolecules* **1994**, *27*, 4145.

(15) (a) Herrington, K. L.; Kaler, E. W.; Miller, D. D.; Zasadzinski, J. A.; Chiruvolu, S. *J. Phys. Chem.* **1993**, *97*, 13792. (b) Talhout, R.; Engberts, J. B. F. N. *Langmuir* **1997**, *13*, 5001. (c) Bergstrom, M.; Pedersen, J. S. *Langmuir* **1998**, *14*, 3754. (d) Frese, Ch.; Ruppert, S.; Schmidt-Lewerkuhne, H.; Wittern, K. P.; Eggers, R.; Fainerman, V. B.; Miller, R. *Phys. Chem. Chem. Phys.* **2004**, *6*, 1592.

(16) Dey, S.; Sasmal, D. K.; Das, D. K.; Bhattacharyya, K. *ChemPhysChem* **2008**, *9*, 2848.

JP1068347